4

Radiative Heat Transfer and Effective Transport Coefficients

Thomas Christen, Frank Kassubek, and Rudolf Gati
ABB Schweiz AG, Corporate Research
Segelhofstrasse 1, CH-5405 Baden-Dättwil
Switzerland

1. Introduction

Heat radiation refers to electromagnetic radiation emitted by thermally excited degrees of freedom of matter. If both the matter and the radiation field are at thermodynamic equilibrium, well-known relations from thermodynamics exist between the temperature T, the characteristic radiation frequency ν, the energy density $E^{(eq)}$, and the pressure $p_{\rm rad}$ of the radiation field. These are Wien's displacement law, $\nu = 5.88 \cdot 10^{10} T$ (ν in Hz and T in K), the caloric equation of state, $E^{(eq)} = 7.57 \cdot 10^{-16} T^4$ (in J/m^3), and the thermal (or thermodynamic) equation of state, $p_{\rm rad} = E^{(eq)}/3$. It is then straight-forward to derive the Stefan-Boltzmann law for the power emitted by a black body, $Q = 5.67 \cdot 10^{-8} T^4$ in units of W/m^2 (cf. Landau & Lifshitz (2005)). In typical applications, heat radiation is relevant in the frequency range of $10^{11} - 10^{16}$ Hz, including the upper part of the microwave band, the infrared, the visible light, and the lower part of the ultra-violet band.

In many cases, be it for engineering purposes like electric arc radiation modelling, or related fundamental scientific problems like in stellar physics, radiation is usually not at thermal equilibrium. The present chapter of this book aims to give a focused overview on the theory of radiative heat transfer, i.e., energy transport by heat radiation that can be in a general nonequilibrium state, while matter is at local thermodynamic equilibrium. With emphasis on models based on partial differential equations for the radiation energy density, heat flux, and (if necessary) higher order moments, we will particularly discuss a powerful method for the determination of effective transport coefficients, which has been recently developed by Christen & Kassubek (2009). General monographs on radiative transfer are given by Chandrasekhar (1960), Siegel & Howell (1992), and Modest (2003), to mention a few.

In Sect. 2 the basic definitions and equations for radiative heat transfer will be introduced. There are two equivalent descriptions of radiation, either in terms of the *specific radiation intensity* (or *radiance*), $I_\nu(\mathbf{x},\mathbf{\Omega},t)$, or the *photon distribution function*, $f_\nu(\mathbf{x},\mathbf{\Omega},t)$. Here, t, $\mathbf{x}$, ν, and $\mathbf{\Omega}$ denote time, position, frequency, and direction (normalized wave-vector), respectively. Frequency dependence will always be indicated by an index ν. The associated transport equations for I_ν and f_ν are named the *radiative transfer equation (RTE)* and the *Boltzmann transport equation (BTE)*, respectively. The number of photons in the volume element $d^3\mathbf{x}$ at position $\mathbf{x}$ and time t, in the frequency band $d\nu$ at ν, and in direction $\mathbf{\Omega}$ within the solid angle $d\mathbf{\Omega}$ equals $f_\nu(\mathbf{x},\mathbf{\Omega},t)\, d^3\mathbf{x}\, d\nu\, d\mathbf{\Omega}$. The intensity is then given by $I_\nu(\mathbf{x},\mathbf{\Omega},t) = ch\nu f_\nu$, where $h\nu$ is the photon energy, $h = 6.626 \cdot 10^{-34}$ Js is Planck's constant, and $c = 2.998 \cdot 10^8$ m/s is the

vacuum velocity of light (cf. Tien (1968)). I_ν is the energy current density per solid angle in direction $\mathbf{\Omega}$.

The RTE (or BTE) is an integro-differential equation for I_ν (or f_ν) in the 6-dimensional phase space corresponding to position, frequency, and direction, and describes the temporal change of I_ν (or f_ν) due to emission, absorption, and scattering by the matter. Finding an appropriate solution is generally a highly sophisticated task, and can be significantly impeded by a complicated frequency dependence of the radiation-matter interaction. Moreover, radiation problems in science and engineering often require a self-consistent solution of the coupled equations for radiation and matter. For instance, a treatment of radiation in hot gases or plasma involves, besides the RTE, the gas-dynamic balance equations for mass, momentum, and energy (or temperature). Despite of the huge progress in computational technologies, an exact solution of the complete set of coupled equations is still unfeasible, except for some especially simple cases. As a consequence, in the course of time a number of methods for approximate solutions of the RTE have been developed. In Sect. 3, we will therefore briefly discuss a selected list of important approximation concepts. Methods based on truncated moment expansions will be emphasized, and the need of a reliable closure method for the determination of the transport coefficients occurring in these equations will be motivated.

In Sect. 4 we will argue that a recently introduced approach for the closure based on entropy production rate is superior to other closures used up to date. The theory of radiation in thermal equilibrium dates back to seminal work by Planck (1906). In chapter 5 of his book Planck emphasizes that, in modern language, photons, unlike a normal gas of massive particles, do not interact among themselves, but interaction with matter is needed for a relaxation to the thermal equilibrium state. As is often the case in many applications of radiative transport, we will assume that the medium, be it condensed matter, gas, or plasma, is at local thermodynamic equilibrium (LTE) and can thus be described locally by thermodynamic quantities like temperature, chemical potential, and the same. It is then the equilibration process of the photon gas to this LTE state that determines the details of the heat transfer by radiation in the medium. As is well-known from thermodynamics, equilibration is related to entropy production, which plays an important role in understanding the behavior of nonequilibrium radiation (cf. Oxenius (1966) and Kröll (1967)). In fact, various authors have shown that the state of radiation is often related to optima of the entropy production rate. Whether the optimum is a maximum or a minimum, depends on the specific details of the system under consideration, particularly on convexity properties of the optimization problem, and particularly, the constraints. For instance, Essex (1984) has shown that the entropy production rate is minimal in a gray atmosphere in local radiative equilibrium. Later on Essex (1997) applied his approach also to neutrino radiation. Würfel & Ruppel (1985) and Kabelac (1994) discussed entropy production rate maximization by introducing an effective chemical potential of the photons, related to their interaction with matter. Santillan et al. (1998) showed that for a constraint of fixed radiation power, black bodies maximize the entropy production rate.

The underlying reason for the success of entropy production rate principles has been recognized already by Kohler (1948), who has shown that the stationary solution of the BTE that is linearized at the equilibrium distribution, generally satisfies a variational principle for the entropy production rate. Kohler's principle has been widely used to determine linear transport coefficients (cf. Ziman (1956) and refs. cited in Martyushev (2006)). The important property of the RTE (or the BTE for photons) is its linearity over the *whole* nonequilibrium range, provided the interaction with the LTE-medium consists of single-photon processes

only. This linearity is thus not an approximation as it was in Kohler's work, but holds for arbitrarily large deviations from thermal equilibrium of the photon gas. The absence of interaction between photons is thus the reason for the success of the concept beyond small deviations of f_ν from equilibrium. Consequently, the entropy production rate is the appropriate basis for the determination of the nonequilibrium distribution I_ν (or f_ν) and the effective transport coefficients for radiative heat transfer in the framework of a truncated moment expansion. In Sect. 5 the transports coefficients, i.e., the effective absorption constants and the Eddington factor, are calculated for some specific examples. A practical reason for using moment equations for modelling radiative transfer is the convenience of having a set of structurally similar equations for the simulation of the complete radiation-hydrodynamics problem. Both the hydrodynamic equations for matter and the moment equations for radiation are hyperbolic partial differential equations and can thus be solved on the same footing. Sect. 5.4 gives some remarks on the requirement of hyperbolicity. For numerical simulations boundary conditions must be specified, these will be discussed in Sect. 6. Finally, Sect. 7 will then provide some simulation results for a simplified example of electric arc radiation.

2. Basics of radiative heat transfer in matter

The radiation intensity, $I_\nu(\mathbf{\Omega})$, is governed by the radiative transfer equation (RTE),

$$\frac{1}{c}\partial_t I_\nu + \mathbf{\Omega}\cdot\nabla I_\nu = \kappa_\nu(B_\nu - I_\nu) + \sigma_\nu\left(\frac{1}{4\pi}\int_{S^2} d\tilde{\Omega}\, p_\nu(\Omega,\tilde{\Omega})\, I_\nu(\tilde{\Omega}) - I_\nu\right) \ , \tag{1}$$

which has to be solved in a spatial region defined by the physical problem under consideration. Phase coherence and interference effects are disregarded when considering thermal radiation, and we will also neglect polarization effects. The BTE is simply obtained by a replacement of I_ν by f_ν in the RTE. The left hand side gives the total rate of change of $I_\nu(\mathbf{\Omega})$, divided by c, along the propagation direction $\mathbf{\Omega}$. This change must be equal to the expression on the right hand side, which consists of a sum of specific source and sink terms due to the radiation-matter interaction. In the absence of any interaction, e.g., in vacuum, the right hand side vanishes, which describes the so-called (free) streaming limit associated with a radiation beam, or the ballistic propagation of the photons. In the presence of interaction, however, photons are generated by emission and annihilated by absorption, described by $\kappa_\nu B_\nu$ and $-\kappa_\nu I_\nu$, respectively. Here, B_ν is the Planck function for thermal equilibrium,

$$B_\nu = \frac{2h\nu^3}{c^2} n^{(eq)} \ , \tag{2}$$

where

$$n_\nu^{(eq)} = \frac{1}{\exp(h\nu/k_B T) - 1} \tag{3}$$

is the Bose-Einstein distribution for thermal equilibrium photons (cf. Landau & Lifshitz (2005)) with the Boltzmann constant $k_B = 1.381\cdot 10^{-23} J/K$ and the local temperature $T = T(\mathbf{x})$ of the LTE medium. The coefficient κ_ν is the macroscopic spectral absorption coefficient in units of 1/m, and is generally a sum of products of particle densities, absorption cross-sections, factors $[1 - \exp(-h\nu/k_B T)]$, and depends thus not only on frequency but also on the partial pressures of the present particle species and the temperature. Often, opacities referring to κ_ν/ρ are discussed in the literature, where ρ is the mass density of

the matter. The macroscopic κ_ν includes spontaneous as well as induced emission (cf. Tien (1968)). Additionally to inelastic absorption-emission processes, Eq. (1) includes elastic (or so-called coherent or conservative) scattering. Incoming photons of frequency ν from all directions $\tilde{\Omega}$ are scattered with probability $p_\nu(\mathbf{\Omega},\tilde{\mathbf{\Omega}})$ into direction $\mathbf{\Omega}$. It is assumed that the phase-function $p_\nu(\Omega,\tilde{\Omega})$ obeys symmetry relations associated with reciprocity, depends only on the cosine between the directions $\tilde{\mathbf{\Omega}}$ and $\mathbf{\Omega}$ (cf. Chandrasekhar (1960)), and is normalized, $(4\pi)^{-1}\int_{S^2} d\tilde{\Omega}\, p_\nu(\Omega,\tilde{\Omega}) = 1$. Here, the Ω-Integration extends over S^2, which denotes the unit sphere associated with the full solid angle. The strength of the scattering process is quantified by the spectral scattering coefficient σ_ν in units of 1/m. The ratio $\sigma_\nu/(\kappa_\nu+\sigma_\nu)$ gives the probability that a collision event is a scattering process, and is sometimes called the *(single-scattering) albedo*. The mean free path of the photons is the inverse of $\kappa_\nu+\sigma_\nu$.
Because the bracket proportional to σ_ν in Eq. (1) vanishes for $\mathbf{\Omega}$-independent I_ν, the RTE can be written in the simple form

$$\frac{1}{c}\partial_t I_\nu + \mathbf{\Omega}\cdot\nabla I_\nu = \mathcal{L}(B_\nu - I_\nu)\ , \tag{4}$$

where the linear, self-adjoint, positive semi-definite[1] operator $\mathcal{L}$ is defined by the right hand side of Eq. (1) and consists of an algebraic term and an integral term.
The RTE has to be solved with appropriate initial conditions, $I_\nu(\mathbf{x},\mathbf{\Omega},t=0)$, and boundary conditions on the surface of the spatial domain under consideration. Because the RTE is a first order differential equation, the determination of each ray requires the knowledge of $I_\nu(\mathbf{\Omega})$ on the domain surface and in directions $\mathbf{\Omega}$ pointing into the domain. The behavior of the boundary is characterized by the radiation it emits, and the way it reflects impinging radiation. If one denotes the emittance of the boundary at position $\mathbf{x_w}$ by $\epsilon(\mathbf{x_w})$, the reflectivity by $r(\mathbf{x_w})$, and the normal vector of the boundary surface by $\mathbf{n}(\mathbf{x_w})$, the boundary condition generally reads (cf. Modest (2003))

$$I_\nu(\mathbf{x_w},\mathbf{\Omega},t) = \epsilon(\mathbf{x_w})B_\nu(\mathbf{x_w}) + \int_{\mathbf{n}(\mathbf{x_w})\cdot\tilde{\mathbf{\Omega}}\le 0} d\tilde{\mathbf{\Omega}}\mid \mathbf{n}(\mathbf{x_w})\cdot\tilde{\mathbf{\Omega}}\mid r(\mathbf{x_w},\mathbf{\Omega},\tilde{\mathbf{\Omega}})I_\nu(\mathbf{x_w},\tilde{\mathbf{\Omega}},t)\ . \tag{5}$$

The integration runs over all $\tilde{\mathbf{\Omega}}$ associated with radiation coming from the bulk domain towards the surface, while $\mathbf{\Omega}$ is pointing into the domain. For a smooth surface where a normal vector $\mathbf{n}(\mathbf{x_w})$ can be defined, this solid angle corresponds to half of the sphere S^2. This boundary condition can be simplified for special limit cases. For instance, a black surface has $r=0$ and $\epsilon=1$, a diffusively reflecting surface has $r(\mathbf{x_w},\mathbf{\Omega},\tilde{\mathbf{\Omega}}) = r(\mathbf{x_w})/\pi$, and a specularly reflecting surface has $r(\mathbf{x_w},\mathbf{\Omega},\tilde{\mathbf{\Omega}}) \propto \delta(\mathbf{\Omega_s}-\tilde{\mathbf{\Omega}})$, where $\mathbf{\Omega_s} = \mathbf{\Omega} - 2(\mathbf{\Omega}\cdot\mathbf{n})\mathbf{n}$ is the direction from which the ray must hit the surface in order to travel into the direction of $\mathbf{\Omega}$ after specular reflection.
We conclude this section by listing the basic equations for the LTE matter to which radiation is coupled. In general, LTE implies that at each point in space, the caloric and thermodynamic equations of state are locally valid. The respective equations relate the specific energy $e = e(\rho,T)$ and the pressure $p = p(\rho,T)$ to the mass density ρ and the temperature T of the matter. The spatio-temporal dynamics of the thermodynamic variables and, if relevant, the flow velocity $\mathbf{u}$, is then given by the hydrodynamic balance equations for mass, momentum,

[1] Note that a negative eigenvalue would immediately lead to an instability.

and energy. For a single component (non-relativistic) medium

$$\partial_t \rho + \nabla \cdot (\rho \mathbf{u}) = \dot{\rho}, \tag{6}$$

$$\partial_t (\rho \mathbf{u}) + \nabla \cdot \mathbf{\Pi}_{\mathrm{mat}} = \mathbf{f}, \tag{7}$$

$$\partial_t (\rho e_{\mathrm{tot}}) + \nabla \cdot \mathbf{j_e} = W, \tag{8}$$

where $\mathbf{\Pi}_{\mathrm{mat}}$, $\mathbf{j_e}$, and $e_{\mathrm{tot}} = e + \mathbf{u}^2/2$ are the momentum stress tensor, the energy flow density, and the total energy density. Together with the equations of state, Eqs. (6)-(8) constitute seven equations for the seven variables ρ, p, T, e, and $\mathbf{u}$. The right hand sides, $\dot{\rho}$, $\mathbf{f}$, and W are the mass source density, the force density, and the heat power density, respectively. The effect of radiation on matter may occur in these three source terms. For instance, a mass source may appear at a solid wall due to ablation by radiation (see, e.g. Christen (2007)), and the radiation pressure may act as a force (cf. Mihalas & Mihalas (1984)). These two effects are often negligible in engineering applications or are important only in special cases, like ablation arcs as discussed by Seeger et al. (2006). However, the heat exchange described by W can in general not be disregarded, and will play an important role in the theory below. The back-coupling of the matter on radiation, as mentioned before, occurs in the expressions on the right hand side of Eq. (1), which depend generally on ρ (or p) and T. An extensive monograph on radiation hydrodynamics is provided by Mihalas & Mihalas (1984), and a short introduction that fits well to the present chapter is given by the lecture notes of Pomraning (1982).

3. Approximation methods

The extreme difficulties to solve the RTE exactly for real systems caused the development of various approximation methods. There are two additional reasons for the use of approximations. First, in many cases the behavior of the matter is of interest, while it is sufficient to consider the radiation as a means of (nonlocal) interaction; hence only the radiative heat flux is needed, which enters the power balance equation for the matter via the heat power density W. As W equals the negative divergence of the radiation energy flux density, a radiation model would be convenient that is confined to this flux and to the lower order moments, which is here a single one, namely the radiation energy density. Secondly, radiation often behaves in two different specific ways. In a transparent medium absorption and scattering are weak, and radiation propagates as beams; full absence of interaction with matter refers to the so-called *free streaming limit*. In an opaque medium, on the other hand, absorption, emission and/or scattering is strong, and the radiation diffuses isotropically. In the extreme diffusive limit the *Rosseland diffusion approximation* applies, where radiative transfer is modelled by an effective heat conductivity of the matter (cf. Siegel & Howell (1992)) given by $16\sigma_{SB}T^3/3\sigma_F^{(\mathrm{eff})}$. Here $\sigma_{SB} = 2\pi^5 k_B^4/15h^3c^2 = 5.67 \cdot 10^{-8}\,\mathrm{W/m^2K^4}$ is the Stefan-Boltzmann constant and $\sigma_F^{(\mathrm{eff})}$ is the Rosseland mean absorption to be discussed later. For the two behaviors a ballistic (beam-like) and a diffusive description, respectively, are the appropriate 'zero order' models with effective transport coefficients, and deviations from the limits may be treated by corrections. Models based on one of these two limit cases can strongly reduce the computational effort. However, in many real systems radiative transfer is in between these limits such that more sophisticated methods must be involved.

In the following, a short list of some relevant approximation methods is given. The selection is not complete, as other approaches exist, like ray tracing and radiosity-irradiosity methods (Rey (2006)), or some rather heuristic methods like the $P_{1/3}$-approximation discussed by

Olson et al. (2000) and Simmons & Mihalas (2000). Furthermore, we will not discuss the issue of discretization methods concerning position space like finite differences, volumes, or elements; although this field would require special recognition (cf. Arridge et al. (2000) and Refs. cited therein), it is beyond the purpose of this chapter. Needless to say that there is not a unique best method, but every approach has its advantages and disadvantages for practical use, and the appropriate choice depends usually on the problem under consideration. Exhaustive overviews can be found, e.g., in Duderstadt & Martin (1979), Siegel & Howell (1992) and literature cited in the following three subsections. Subsequently, we will then focus in subsection 3.4 on approximations based on moment expansions, and particularly on the closure of the moment equations that will be discussed in Sect. 4.

3.1 Net emission

The *net emission approximation* is probably the most simplistic radiation model. It assumes a semi-empirical function $W(T,p,\boldsymbol{\zeta})$ in Eq. (8). Additionally to temperature and pressure, it depends on parameters $\boldsymbol{\zeta}$ of the radiating object. It is sometimes used, for instance, in computational fluid dynamics simulations of electrical arcs (cf. Lowke (1970), Zhang et al. (1987), Seeger et al. (2006)), where the only additional parameter ζ is the arc radius. Although such a description is very convenient in numerical simulations and sometimes even provides useful results, it is obviously oversimplifying and without any rigor. Furthermore, reliable accuracy requires, for the determination of the function $W(T,p,\zeta)$, a parameter study based on a more fundamental radiation model or on elaborate experiments.

3.2 Monte Carlo

Monte Carlo simulations refer to random sampling methods (see, for instance Yang et al. (1995) and Duderstadt & Martin (1979)), which are based on computer simulations of a number of photons. Their deterministic dynamics corresponds to the ballistic motion with speed of light. Emission, absorption, and scattering processes are simulated in a probabilistic way by appropriately determined random numbers for the various processes. Those include, of course, the interaction with boundaries of the spatial domain. Final results, like the radiation intensity, are determined by averages over many photon particles. The Monte Carlo concept is rather simple, which leads to a number of advantages of this method, as discussed by Yang et al. (1995). Efficient applications make use of specifically improved schemes like implicit Monte Carlo or special versions thereof (cf. Brooks & Fleck (1986) and Brooks et al. (2005)).

3.3 Discrete ordinates

The *discrete ordinates method* (*DOM*) considers a finite number of rays passing at every (discrete) space point. If a number N_D of direction vectors $\boldsymbol{\Omega}_k$, $k = 1,...,N_D$ is selected, one has $I_\nu = \Sigma_k I_\nu^{(k)} \delta(\boldsymbol{\Omega} - \boldsymbol{\Omega}_k)$, such that a set of N_D partially coupled RTE-equations for the different directions and frequencies must be solved. The right hand side of these equations, say $\tilde{\mathcal{L}}(B_\nu - I_\nu^{(k)})$, contains not an integral as Eq. (1) but a weighted sum. As reasonable values for N_D in 3-dimensional realistic geometries are at least of the order of 10, the computational effort is still large. For too small N_D an artifact called "ray effect" may occur, referring to spatial oscillations in the energy density. Another error known as "false scattering" or "false diffusion", is due to the discretization of position space and is linked in a certain way to the ray effect as discussed in Rey (2006).
Some further developments based on DOM exist, which make use of a decomposition and

discretization of the angular space into a finite set of directions, i.e. a finite partition of the unit sphere S^2. The methods of *partial characteristics* (Aubrecht & Lowke (1994)) and of *partial moments* (Frank et al. (2006)) are examples, the latter being mentioned again in the next section. Last but not least, we mention that it has been proven that the DOM is equivalent, under certain conditions, to the P-N method (cf. Barichello & Siewert (1998) and Cullen (2001)), which is a special kind of the moment approximations to be discussed in the next subsection.

3.4 Moment expansions

Radiation modelling in terms of moments of the distribution I_ν (or f_ν) is convenient because the radiation is coupled to the LTE matter in Eqs. (6)-(8) via the first three (angular) moments. Moment expansions can be formulated in a rather general manner (cf. Levermore (1996) and Struchtrup (1998)). In the following, we define moments based on I_ν by

$$E = \int_0^\infty d\nu\, E_\nu = \int_0^\infty d\nu \frac{1}{c} \int_{S^2} d\Omega\, I_\nu \ , \tag{9}$$

$$\mathbf{F} = \int_0^\infty d\nu\, \mathbf{F}_\nu = \int_0^\infty d\nu \frac{1}{c} \int_{S^2} d\Omega\, \mathbf{\Omega}\, I_\nu \ , \tag{10}$$

$$\mathbf{\Pi} = \int_0^\infty d\nu\, \mathbf{\Pi}_\nu = \int_0^\infty d\nu \frac{1}{c} \int_{S^2} d\Omega\, \mathbf{\Omega} : \mathbf{\Omega}\, I_\nu \ , \tag{11}$$

$$\ldots = \ldots \ ,$$

with $(\mathbf{\Omega} : \mathbf{\Omega})_{kl} = \Omega_k \Omega_l$. The last line indicates that an infinite number of moments exist in general. E_ν, $\mathbf{F}_\nu$, and $\mathbf{\Pi}_\nu$ are, respectively, the monochromatic energy density, radiative flux, and stress (or pressure) tensor of the radiation. For convenience, the prefactor (c^{-1}) is chosen in all definitions such that the moments have the same units of a spectral energy density. Similarly, E, $\mathbf{F}$, and $\mathbf{\Pi}$ are the spectrally integrated energy density, radiative flux, and pressure tensor. In the present units $F = \mid \mathbf{F} \mid$ has the meaning of energy density associated with the average directed motion of the photons, and E of the total energy density composed of directed and thermal fluctuation parts. Hence, $F \leq \mid E \mid$, which will be important below.
In thermal equilibrium all fluxes vanish. Then $\mathbf{F}_\nu = 0$, the stress tensor is proportional to the unit tensor with diagonal elements $E^{(eq)}/3$, and the energy density is given by

$$E^{(eq)} = \int_0^\infty 4\pi\, d\nu\, B_\nu = \frac{4\sigma_{SB}}{c} T^4 \ . \tag{12}$$

The purpose of a moment expansion is to derive from the RTE or BTE balance equations for the moments, either for each frequency ν, or for groups of frequencies or frequency bands, or for the full, integrated spectral range. Multiplication of the RTE with products and/or powers of Ω_k's, and integration over the solid angle gives for the moments E_ν, $\mathbf{F}_\nu$, etc.

$$\frac{1}{c}\partial_t E_\nu + \nabla \cdot \mathbf{F}_\nu = \frac{1}{c} \int_{S^2} d\Omega\, \mathcal{L}(B_\nu - I_\nu) \ , \tag{13}$$

$$\frac{1}{c}\partial_t \mathbf{F}_\nu + \nabla \cdot \mathbf{\Pi}_\nu = \frac{1}{c} \int_{S^2} d\Omega\, \mathbf{\Omega}\, \mathcal{L}(B_\nu - I_\nu) \ , \tag{14}$$

etc., where only the first two equations are listed for convenience, but the list still contains an infinite number for all moments and for all frequencies. Practical usability calls then for a two-fold approximation. First, the list of moments, and thus moment equations, should be truncated by considering only the N first moment equations. Secondly, the frequency space

should be discretized or partitioned in some way, in order to end up with a finite set. If the spectrum allows a division into a number of well defined frequency bands with approximately constant κ_ν and σ_ν, or a grouping of different frequencies together according to similar values of κ_ν and σ_ν, one can average the equations over such partitions. The associated methods are sometimes named multi-group, multi-band, or multi-bin methods. For details, we refer the reader to Turpault (2005), Ripoll & Wray (2008), Nordborg & Iordanidis (2008), and the literature cited therein. In the following we will consider the equations for the spectrally averaged quantities, which are obtained by integration of Eqs. (13), (14), etc., over frequency

$$\frac{1}{c}\partial_t E + \nabla \cdot \mathbf{F} = P_E = \frac{1}{c}\int_0^\infty d\nu \int_{S^2} d\Omega\, \mathcal{L}(B_\nu - I_\nu) \ , \tag{15}$$

$$\frac{1}{c}\partial_t \mathbf{F} + \nabla \cdot \mathbf{\Pi} = \mathbf{P_F} = \frac{1}{c}\int_0^\infty d\nu \int_{S^2} d\Omega \ , \mathbf{\Omega}\, \mathcal{L}(B_\nu - I_\nu), \tag{16}$$

etc., where the right hand sides define P_E and $\mathbf{P_F}$, etc. These quantities are still functionals of the unknown function I_ν. All moments, on the other hand, are variables that are determined by the full (still infinite) set of partial differential equations, provided reasonable initial and boundary conditions are given.

Now we perform a truncation by using only the first N moment equations. The first N moments would then be determined by the solution of these equations, if the right hand sides (P_E, $\mathbf{P_F}$, etc) and the $N+1$'th moment were known. In the following section we will discuss closure methods that determine these unknowns, which are supposed to be functions of the N moments. Prior, however, we remark that instead of using products of Cartesian coordinates of $\mathbf{\Omega}$, one may equivalently consider a representation in terms of spherical coordinates (θ, ϕ). The radiation density is then expanded in spherical harmonics $Y_l^m(\theta, \phi)$. If truncated, this approximation corresponds to the P-N approximation (cf. Siegel & Howell (1992)). The prominent P-1 approximation (cf. Siegel & Howell (1992)), for instance, refers to a truncation of the Eqs. (13) and (14) (or Eqs. (15) and (16)) after the second equation and considers an isotropic Π_ν (or Π) with diagonal elements equal to $E_\nu/3$ (or $E/3$).

We also mention again the partial moment approximation (cf. Frank et al. (2006)), where the approaches of DOM and moment expansion are combined in a smart way. As the DOM discretizes the angular space in different directions, the partial moment method selects partitions $\mathcal{A}$ of the unit sphere S^2 and defines partial moments $E_\nu^{(\mathcal{A})}$, $\mathbf{F}_\nu^{(\mathcal{A})}$, $\mathbf{\Pi}_\nu^{(\mathcal{A})}$, etc , where the solid angle integration is performed only over $\mathcal{A}$ instead of the whole S^2. The most simple but nontrivial partial moment model refers to the forward and backward traveling waves in a one-dimensional position space, where the integration occurs over the two half-spheres associated with forward and backward directions. According to Frank (2007), this method has several advantages, e.g., it is able to resolve a shock-wave artifact occurring for counter-propagating and interpenetrating radiation beams.

4. Closure approaches

The quality of the moment approximation depends on the number of moments taken into account, and on the specific closure concept. A closure of a truncated moment expansion requires in principle knowledge of I_ν. A simplification occurs if κ_ν, σ_ν, and p_ν are assumed to be constant (gray matter). The right hand sides of the moment equations strongly simplify as they can be directly expressed in terms of these constants and linear expressions of the moments. But in general matter is non-gray, and the absorption and scattering spectra can be extremely complex. Furthermore, the $N+1$'th moment remains still unknown even for gray

matter. In the sequel we will discuss a few practically relevant closure methods. We will then argue that the preferred closure is given by an entropy production principle.
For clarity we will consider the two-moment example; generalization to an arbitrary number of moments is straight-forward. The appropriate number of moments is influenced by the geometry and the optical density of the matter. For symmetric geometries, like plane, cylindrical, or spherical symmetry, less moments are needed than for complex arrangements with shadowing corners, slits, and the same. For optically dense matter, the photons behave diffusive, which can be modelled well by a low number of moments, as will be discussed below. For transparent media, beams, or even several beams that might cross and interpenetrate, may occur, which makes higher order or multipole moments necessary.

4.1 Two-moment example

The unknowns are P_E, $\mathbf{P_F}$, and $\mathbf{\Pi}$, which may be functions of the two moments E and $\mathbf{F}$. For convenience, we will write

$$P_E = \kappa_{\mathrm{E}}^{(\mathrm{eff})}(E^{(eq)} - E) \ , \tag{17}$$

$$\mathbf{P_F} = -\kappa_{\mathrm{F}}^{(\mathrm{eff})}\mathbf{F} \ , \tag{18}$$

where we introduced the effective absorption coefficients $\kappa_{\mathrm{E}}^{(\mathrm{eff})}$ and $\kappa_{\mathrm{F}}^{(\mathrm{eff})}$ that are generally functions of E and $\mathbf{F}$. Because the second rank tensor $\mathbf{\Pi}$ depends only on the scalar E and the vector $\mathbf{F}$, by symmetry reason it can be written in the form

$$\Pi_{nm} = E\left(\frac{1-\chi}{2}\delta_{nm} + \frac{3\chi-1}{2}\frac{F_n F_m}{F^2}\right) \ , \tag{19}$$

where the *variable Eddington factor (VEF)* χ is a function of E and $\mathbf{F}$ and where $\delta_{kl}(=0$ if $k \neq l$ and $\delta_{kl}=1$ if $k=l)$ is the Kronecker delta. Assuming that the underlying matter is isotropic, $\kappa_E^{(\mathrm{eff})}$, $\kappa_F^{(\mathrm{eff})}$, and χ can be expressed as functions of E and

$$v = \frac{F}{E} \tag{20}$$

with $F = \mid \mathbf{F} \mid$. Obviously it holds $0 \leq v \leq 1$, with $v = 1$ corresponding to a fully directed radiation beam (free streaming limit). According to Pomraning (1982), the additional E-dependence of suggested or derived VEFs often appears via an effective E-dependent single scattering albedo, which equals, e.g. for gray matter, $(\kappa E^{(eq)} + \sigma E)/(\kappa + \sigma)E$.
The task of a closure is to determine the *effective transport coefficients*, i.e., *effective mean absorption coefficients* $\kappa_E^{(\mathrm{eff})}$, $\kappa_F^{(\mathrm{eff})}$, and the VEF χ as functions of E and F (or v). This task is of high relevance in various scientific fields, from terrestrial atmosphere physics and astrophysics to engineering plasma physics.

4.2 Exact limits and interpolations

In limit cases of strongly opaque and strongly transparent matter, analytical expressions for the effective absorption coefficients are often used, which can be determined in principle from basic gas properties (see, e.g., AbuRomia & Tien (1967) and Fuss & Hamins (2002)). In an optically dense medium radiation behaves diffusive and isotropic, and is near equilibrium with respect to LTE-matter. The effective absorption coefficients are given by the so-called

Rosseland average or *Rosseland mean* (cf. Siegel & Howell (1992))

$$\kappa_E^{(\mathrm{eff})} = \langle \kappa_\nu \rangle_{\mathrm{Ro}} := \frac{\int_0^\infty d\nu\, \nu^4 \partial_\nu n_\nu^{(eq)}}{\int_0^\infty d\nu\, \nu^4 \kappa_\nu^{-1} \partial_\nu n_\nu^{(eq)}} \ , \tag{21}$$

where ∂_ν denotes differentiation with respect to frequency, and

$$\kappa_F^{(\mathrm{eff})} = \langle \kappa_\nu + \sigma_\nu \rangle_{\mathrm{Ro}} \ . \tag{22}$$

The Rosseland mean is an average of inverse rates, i.e., of scattering times, and must thus be associated with consecutive processes. A hand-waving explanation is based on the strong mixing between different frequency modes by the many absorption-emission processes in the optically dense medium due to the short photon mean free path.
Isotropy of $\mathbf{\Pi}$ implies for the Eddington factor $\chi = 1/3$. Indeed, because $\sum \Pi_{kk} = E$, one has then $\mathbf{\Pi}_{kl} = \delta_{kl} E/3$. With these stipulations, Eqs. (15) and (16) are completely defined and can be solved.
In a strongly scattering medium ($\sigma_\nu \gg \kappa_\nu$), where $\mathbf{F}$ relaxes quickly to its quasi-steady state, one may further assume $\mathbf{F} = -\nabla E/3\kappa_F^{(\mathrm{eff})}$ for appropriate time scales. Hence Eq. (15) becomes

$$\frac{1}{c}\partial_t E - \nabla \cdot \left(\frac{\nabla E}{3\kappa_F^{(\mathrm{eff})}} \right) = \kappa_E^{(\mathrm{eff})} (E^{(eq)} - E) \ , \tag{23}$$

which has the form of a reaction-diffusion equation. For engineering applications, E often relaxes much faster than all other hydrodynamic modes of the matter, such that the time derivative of Eq. (23) can be disregarded by assuming full quasi-steady state of the radiation. Equation (23) is then equivalent to an effective steady state gray-gas P-1 approximation.

For transparent media, in which the radiation beam interacts weakly with the matter, the Planck average is often used,

$$\langle \kappa_\nu \rangle_{\mathrm{Pl}} = \frac{\int_0^\infty d\nu\, \nu^3 \kappa_\nu n_\nu^{(eq)}}{\int_0^\infty d\nu\, \nu^3 n_\nu^{(eq)}} \ . \tag{24}$$

In contrast to the Rosseland mean, the Planck mean averages the rates and can thus be associated with parallel processes, because scattering is weak and there is low mixing between different frequency modes. In contrast to the Rosseland average, the Planck average is dominated by the largest values of the rates. Although in this case radiation is generally not isotropic, there are special cases where an isotropic $\mathbf{\Pi}$ can be justified; an example discussed below is the $v \to 0$ limit in the emission limit $E/E^{(eq)} \to 0$. But note that $\chi = 1$ often occurs in transparent media, and consideration of the VEF is necessary.

In the general case of intermediate situations between opaque and transparent media, heuristic interpolations between fully diffusive and beam radiation are sometimes performed. Effective absorption coefficients have been constructed heuristically by Patch (1967), or by Sampson (1965) by interpolating Rosseland and Planck averages.
The consideration of the correct stress tensor is even more relevant, because the simple $\chi = 1/3$ assumption can lead to the physical inconsistency $v > 1$. A common method to

solve this problem is the introduction of flux limiters in diffusion approximations, where the effective diffusion constant is assumed to be state-dependent (cf. Levermore & Pomraning (1981), Pomraning (1981), and Levermore (1984), and Refs. cited therein). A similar approach in the two-moment model is the use of a heuristically constructed VEF. A simple class of flux-limiting VEFs is given by

$$\chi = \frac{1+2v^j}{3} \ , \tag{25}$$

with positive j. These VEFs depend only on v, but not additionally separately on E. The cases $j = 1$ and $j = 2$ are attributed to Auer (1984) and Kershaw (1976), respectively. While the former strongly simplifies the moment equations by making them piecewise linear, the latter fits quite well to realistic Eddington factors, particularly for gray matter, but with the disadvantage of introducing numerical difficulties.

4.3 Maximum entropy closure

An often used closure is based on *entropy maximization* (cf. Minerbo (1978), Anile et al. (1991), Cernohorsky & Bludman (1994), and Ripoll et al. (2001)).[2] This closure considers the local radiation entropy as a functional of I_ν. The entropy of radiation is defined at each position $\mathbf{x}$ and is given by (cf. Landau & Lifshitz (2005), Oxenius (1966), and Kröll (1967))

$$S_{\mathrm{rad}}[I_\nu] = -k_B \int d\Omega\, d\nu \frac{2\nu^2}{c^3} \left(n_\nu \ln n_\nu - (1+n_\nu)\ln(1+n_\nu)\right), \tag{26}$$

where

$$n_\nu(\mathbf{x},\mathbf{\Omega}) = \frac{c^2 I_\nu}{2h\nu^3} \tag{27}$$

is the photon distribution for the state $(\nu,\mathbf{\Omega})$.[3] At equilibrium (27) is given by (3). I_ν is then determined by maximizing $S_{\mathrm{rad}}[I_\nu]$, subject to the constraints of fixed moments given by Eqs. (9), (10) etc. This provides I_ν as a function of ν, Ω, E and $\mathbf{F}$. If restricted to the two-moment approximation, the approach is sometimes called the M-1 closure. It is generally applicable to multigroup or multiband models (Cullen & Pomraning (1980), Ripoll (2004), Turpault (2005), Ripoll & Wray (2008)) and partial moments (Frank et al. (2006), Frank (2007)), as well as for an arbitrarily large number of (generalized) moments (Struchtrup (1998)). It is clear that this closure can equally be applied to particles obeying Fermi statistics (see Cernohorsky & Bludman (1994) and Anile et al. (2000)).

Advantages of the maximum entropy closure are the mathematical simplicity and the mitigation of fundamental physical inconsistencies (Levermore (1996) and Frank (2007)). In particular, there is a natural flux limitation by yielding a VEF with correct limit behavior in both isotropic radiation ($\chi \to 1/3$) and free streaming limit ($\chi \to 1$):

$$\chi_{\mathrm{ME}} = \frac{5}{3} - \frac{4}{3}\sqrt{1-\frac{3}{4}v^2} \tag{28}$$

that depends only on v. Furthermore, because the optimization problem is convex[4], the uniqueness of the solution is ensured and, as shown by Levermore (1996), the moment

[2] In part of the more mathematically oriented literature, the entropy is defined with different sign and the principle is called "minimum entropy closure".

[3] Note the simplified notation of a single integral symbol $\int$ in Eq. (26) and in the following, which is to be associated with full frequency and angular space.

[4] Convexity refers here to the mathematical entropy definition with a sign different from Eq. (26).

equations are hyperbolic, which is important because otherwise the radiation model would be physically meaningless. The main disadvantage is that the maximum entropy closure is unable to give the correct Rosseland mean in the near-equilibrium limit, and can thus not be correct. For example, for $\sigma_\nu \equiv 0$ the near-equilibrium effective absorption coefficients are given by (Struchtrup (1996))

$$\langle \kappa_\nu \rangle_{\mathrm{ME}} = \frac{\int_0^\infty d\nu\, \nu^4 \kappa_\nu \partial_\nu n_\nu^{(eq)}}{\int_0^\infty d\nu\, \nu^4 \partial_\nu n_\nu^{(eq)}} \ , \tag{29}$$

which is a Planck-like mean that averages κ_ν instead of averaging its inverse. It is only seemingly surprising that the maximum entropy closure is wrong even close to equilibrium. This closure concept must fail in general, as Kohler (1948) has proven that for the linearized BTE the *entropy production rate*, rather than the *entropy*, is the quantity that must be optimized. Both approaches lead of course to the correct equilibrium distribution. But the quantity responsible for transport is the first order deviation $\delta I_\nu = I_\nu - B_\nu$, which is determined by the entropy production and not by the entropy. Moreover, it is obvious that Eq. (26) is explicitly independent of the radiation-matter interaction. Consequently, the distribution resulting from entropy maximization cannot depend explicitly on the spectral details of κ_ν and σ_ν, which must be wrong in general. A critical discussion of the maximum entropy production closure was already given by Struchtrup (1998); he has shown that only a large number of moments generalized to higher powers in frequency up to order ν^4, are able to reproduce the correct result in the weak nonequilibrium case. Consequently, despite of its ostensible mathematical advantages, we propose to reject the maximum entropy closure for the moment expansion of radiative heat transfer. A physically superior method based on the entropy production rate will be discussed in the next subsection.

4.4 Minimum entropy production rate closure

As mentioned, Kohler (1948) has proven that a minimum entropy production rate principle holds for the linearized BTE. The application of this principle to moment expansions has been shown by Christen & Kassubek (2009) for the photon gas and by Christen (2010) for a gas of independent electrons. The formal procedure is fully analogous to the maximum entropy closure, but the functional to be minimized is in this case the *total entropy production rate*, which consist of two parts associated with the radiation field, i.e., the photon gas, and with the LTE matter. The latter acts as a thermal equilibrium bath. The two success factors of the application of this closure to radiative transfer are first that the RTE is linear not only near equilibrium but in the whole range of I_ν (or f_ν) values, and secondly that the entropy expression Eq. (26) is valid also far from equilibrium (cf. Landau & Lifshitz (2005)).

In order to derive the expression for the entropy production rate, $\dot{S}$, one can consider separately the two partial (and spatially local) rates $\dot{S}_{\mathrm{rad}}$ and $\dot{S}_{\mathrm{m}}$ of the radiation and the medium, respectively (cf. Struchtrup (1998)). $\dot{S}_{\mathrm{rad}}$ is obtained from the time-derivative of Eq. (26), use of Eq. (1), and writing the result in the form $\partial_t S_{\mathrm{rad}} + \nabla \cdot \mathbf{J}_S = \dot{S}_{\mathrm{rad}}$ with

$$\dot{S}_{\mathrm{rad}}[I_\nu] = -k_B \int d\nu\, d\Omega \frac{1}{h\nu} \ln\left(\frac{n_\nu}{1+n_\nu}\right) \mathcal{L}(B_\nu - I_\nu) \ , \tag{30}$$

where n_ν is given by Eq. (27). $\mathbf{J}_S$ is the entropy current density, which is not of further interest in the following. The entropy production rate of the LTE matter, $\dot{S}_{\mathrm{mat}}$, can be derived from the fact that the matter can be considered locally as an equilibrium bath with temperature $T(\mathbf{x})$.

Energy conservation implies that W in Eq. (8) is related to the radiation power density in Eq. (15) by $W = -P_E$. The entropy production rate (associated with radiation) in the local heat bath is thus $\dot{S}_{\rm mat} = W/T = -P_E/T$. Equation (3) implies $h\nu/k_BT = \ln(1+1/n_\nu^{(eq)})$, and one obtains

$$\dot{S}_{\rm mat}[I_\nu] = -k_B \int d\nu\, d\Omega \frac{1}{h\nu} \ln\left(\frac{1+n_\nu^{(eq)}}{n_\nu^{(eq)}}\right) \mathcal{L}(B_\nu - I_\nu) \ . \tag{31}$$

The total entropy production rate $\dot{S} = \dot{S}_{\rm rad} + \dot{S}_{\rm mat}$ is

$$\dot{S}[I_\nu] = \int_0^\infty d\nu\, \dot{S}_\nu = -k_B \int d\nu\, d\Omega \frac{1}{h\nu} \ln\left(\frac{n_\nu(1+n_\nu^{(eq)})}{n_\nu^{(eq)}(1+n_\nu)}\right) \mathcal{L}(B_\nu - I_\nu) \ . \tag{32}$$

The closure receipt prescribes to minimize $\dot{S}[I_\nu]$ by varying I_ν subject to the constraints that the moments E, $\mathbf{F}$, ... etc. are fixed. The solution I_ν of this constrained optimization problem depends on the values E, $\mathbf{F}$, ... The number N of moments to be taken into account is in principle arbitrary, but we still restrict the discussion to E and $\mathbf{F}$. After introducing Lagrange parameters λ_E and $\boldsymbol{\lambda}_F$, one has to solve

$$\delta_{I_\nu}\left[\dot{S}[I_\nu] - \lambda_E\left(E - \frac{1}{c}\int d\nu d\Omega\, I_\nu\right) - \boldsymbol{\lambda}_F \cdot \left(\mathbf{F} - \frac{1}{c}\int d\nu d\Omega\, \mathbf{\Omega}\, I_\nu\right)\right] = 0 \quad , \tag{33}$$

where δ_{I_ν} denotes the variation with respect to I_ν. The solution of this minimization problem provides the nonequilibrium state I_ν.

5. Effective transport coefficients

We will now calculate the effective transport coefficients $\kappa_E^{(\rm eff)}$, $\kappa_F^{(\rm eff)}$, and the Eddington factor χ with the help of the entropy production rate minimization closure. We assume $\mathbf{F} = (0,0,F)$ in x_3-direction, use spherical coordinates (θ,ϕ) in Ω-space, such that I_ν is independent of the azimuth angle ϕ. For simplicity, we consider isotropic scattering with $p(\mathbf{\Omega},\tilde{\mathbf{\Omega}}) = 1$, although it is straightforward to consider general randomly oriented scatterers with the phase function p_ν being a series in terms of Legendre polynomials $P_n(\mu)$. Here, we introduced the abbreviation $\mu = \cos(\theta)$. With $d\mathbf{\Omega} = 2\pi\sin(\theta)d\theta = -2\pi d\mu$, the linear operator $\mathcal{L}$, acting on a function $\varphi_\nu(\mu)$, can be written as

$$\mathcal{L}\varphi_\nu = \kappa_\nu\varphi_\nu(\mu) + \sigma_\nu\left(\varphi_\nu(\mu) - \frac{1}{2}\int_{-1}^{1} d\tilde{\mu}\, \varphi_\nu(\tilde{\mu})\right) \ , \tag{34}$$

which has an eigenvalue κ_ν with eigenfunction $P_0(\mu)$ and (degenerated) eigenvalues $\kappa_\nu + \sigma_\nu$ for all higher order Legendre polynomials $P_n(\mu)$, $n = 1,2,...$. In the following two subsections we focus first on limit cases that can be analytically solved, namely radiation near equilibrium (leading order in $E - E^{(eq)}$ and F), and the emission limit (leading order in E, while $0 \le F \le E$). In the remaining subsections the general behavior obtained from numerical solutions and a few mathematically relevant issues will be discussed.

5.1 Radiation near equilibrium

Radiation at thermodynamic equilibrium obeys $I_\nu = B_\nu$ and $F = 0$. Near equilibrium, or weak nonequilibrium, refers to linear order in the deviation $\delta I_\nu = I_\nu - B_\nu$. Higher order corrections of the moments $E = E^{(eq)} + \delta E$ and $F = \delta F$ are neglected. Because the stress tensor is an

even function of δI_ν, $\chi = 1/3$ remains still valid in the linear nonequilibrium region (except for the singular case of Auer's VEF with $j = 1$). We will now show that, in contrast to the entropy maximization closure, the entropy production minimization closure yields the correct Rosseland radiation transport coefficients (cf. Christen & Kassubek (2009)).
For isotropic scattering it is sufficient to take into account the first two Legendre polynomials, 1 and μ: $\delta I_\nu = c_\nu^{(0)} + c_\nu^{(1)}\mu$, with μ-independent $c_\nu^{(0,1)}$ that must be determined. Equations (9) and (10) yield

$$\delta E_\nu = \frac{2\pi}{c}\int_{-1}^{1} d\mu\,(c_\nu^{(0)} + c_\nu^{(1)}\mu) = \frac{4\pi}{c}c_\nu^{(0)}, \tag{35}$$

$$\delta F_\nu = \frac{2\pi}{c}\int_{-1}^{1} d\mu\,(c_\nu^{(0)} + c_\nu^{(1)}\mu)\mu = \frac{4\pi}{3c}c_\nu^{(1)}, \tag{36}$$

and from Eq. (32)

$$\dot{S}_\nu = \frac{2k_B\pi c^2}{h^2\nu^4 n_\nu^{(eq)}(1+n_\nu^{(eq)})}\left(\kappa_\nu (c_\nu^{(0)})^2 + \frac{1}{3}(\kappa_\nu+\sigma_\nu)(c_\nu^{(1)})^2\right)\ . \tag{37}$$

Minimization of $\dot{S}_\nu$ with respect to $c_\nu^{(0,1)}$ with constraints $\delta E = \int d\nu \delta E_\nu$ and $\delta F = \int d\nu \delta F_\nu$ leads to

$$c_\nu^{(0)} = \frac{c\nu^4\partial_\nu n_\nu^{(eq)}}{4\pi\kappa_\nu\int d\nu\,\nu^4\kappa_\nu^{-1}\partial_\nu n_\nu^{(eq)}}\delta E, \tag{38}$$

$$c_\nu^{(1)} = \frac{3c\nu^4\partial_\nu n_\nu^{(eq)}}{4\pi(\kappa_\nu+\sigma_\nu)\int d\nu\,\nu^4(\kappa_\nu+\sigma_\nu)^{-1}\partial_\nu n_\nu^{(eq)}}\delta F\ , \tag{39}$$

where we made use of the relation $\partial_\nu n_\nu^{(eq)} = n_\nu^{(eq)}(1+n_\nu^{(eq)})h/k_BT$. As δI_ν is known to leading order in δE and δF, the transport coefficients can be calculated. One finds

$$\kappa_E^{(\mathrm{eff})} = \frac{2\pi}{c}\int d\nu d\mu\,\frac{\mathcal{L}(\delta I_\nu)}{\delta E} = \frac{4\pi}{c}\int d\nu\kappa_\nu\frac{c_\nu^{(0)}}{\delta E} = \langle\kappa_\nu\rangle_{\mathrm{Ro}}, \tag{40}$$

$$\kappa_F^{(\mathrm{eff})} = \frac{2\pi}{c}\int d\nu d\mu\,\mu\,\frac{\mathcal{L}(\delta I_\nu)}{\delta F} = \frac{4\pi}{c}\int d\nu(\kappa_\nu+\sigma_\nu)\frac{c_\nu^{(1)}}{3\delta F} = \langle\kappa_\nu+\sigma_\nu\rangle_{\mathrm{Ro}}\ , \tag{41}$$

hence the effective absorption coefficients are given by the Rosseland averages Eqs. (21) and (22). Similarly, it is shown that $\Pi_{kl} = (E/3)\delta_{kl}$. This proves that the minimum entropy production rate closure provides the correct radiative transport coefficients near equilibrium.

5.2 Emission limit

While the result of the previous subsection was expected due to the general proof by Kohler (1948), the emission limit is another analytically treatable case, which is, however, far from equilibrium. It is characterized by a photon density much smaller than the equilibrium density, hence $I_\nu \ll B_\nu$, i.e., $E \ll E^{(eq)}$, i.e., emission strongly predominates absorption. To leading order in n_ν, the entropy production rate becomes

$$\dot{S}_\nu = -2\pi k_B\int_{-1}^{1} d\mu\,\frac{\kappa_\nu B_\nu}{h\nu}\ln(n_\nu) \tag{42}$$

such that constrained optimization gives

$$I_\nu = \frac{2k_B}{c}\frac{\nu^2\kappa_\nu}{\lambda_E+\lambda_F\mu}n_\nu^{(eq)} \ , \tag{43}$$

with Lagrange parameters λ_E and λ_F. The μ-integration in Eqs. (9) and (10) can be performed analytically, yielding

$$E = \frac{k_B\mathcal{T}(\kappa_\nu)}{c^2\lambda_F}\ln\left(\frac{\lambda_E+\lambda_F}{\lambda_E-\lambda_F}\right), \tag{44}$$

$$F = \frac{k_B\mathcal{T}(\kappa_\nu)}{c^2\lambda_F}\left(2-\frac{\lambda_E}{\lambda_F}\ln\left(\frac{\lambda_E+\lambda_F}{\lambda_E-\lambda_F}\right)\right) \ , \tag{45}$$

where we introduced

$$\mathcal{T}(\kappa_\nu) = 4\pi\int_0^\infty d\nu\,\nu^2\kappa_\nu n_\nu^{(eq)} \ . \tag{46}$$

Up to leading order in I_ν, one finds by performing the integration analogous to Eqs. (40) and (41)

$$\kappa_E^{(\mathrm{eff})} = \langle\kappa_\nu\rangle_{\mathrm{Pl}} \quad \text{and} \quad \kappa_F^{(\mathrm{eff})} = \frac{\mathcal{T}(\kappa_\nu(\kappa_\nu+\sigma_\nu))}{\mathcal{T}(\kappa_\nu)} \ . \tag{47}$$

As one expects, in the emission limit the effective absorption coefficients are Planck-like, i.e., a direct average rather than an average of the inverse rates like Rosseland averages. The Eddington factor can be obtained from $\Pi_{33} = \chi E$ by calculating

$$\Pi_{33} = \frac{2\pi}{c}\int_0^\infty d\nu\int_{-1}^1 d\mu\,\mu^2 I_\nu \ , \tag{48}$$

which leads to

$$\chi(v) = -\frac{\lambda_E}{\lambda_F}v \ , \tag{49}$$

where the ratio of the Lagrange parameters, and thus also the VEF, depends only on $v = F/E$. This can be seen if one divides Eq. (44) by (45). For small v, the expansion of Eqs. (44) and (45) gives $\lambda_E/\lambda_F = -1/3v$, in accordance with the isotropic limit. In the free streaming limit, $v \to 1$ from below, it holds $\lambda_F \to -\lambda_E$, which follows from $\ln(Z) = 2 - \lambda_E\ln(Z)/\lambda_F$ with $Z = (\lambda_E+\lambda_F)/(\lambda_E-\lambda_F)$ obtained from equalizing (44) with (45).
For arbitrary v the Eddington factor in the emission limit can easily be numerically calculated by division of Eq. (44) by Eq. (45), and parameterizing v and χ with λ_F/λ_E. The result will be shown below in Fig. 4 a). It turns out that the difference to other VEFs often used in literature is quantitatively small.
While Christen & Kassubek (2009) disregarded scattering, it is included here. For strong scattering $\sigma_\nu \gg \kappa_\nu$, Eq. (47) implies that the effective absorption coefficient $\kappa_F^{(\mathrm{eff})}$ of the radiation flux is given by a special average of σ_ν where κ_ν enters in the weight function. In particular, for frequencies where κ_ν vanishes, there is no elastic scattering contribution to the average in this limit. This can be understood by the absence of photons with this frequency in the emission limit.

5.3 General nonequilibrium case

The purpose of this subsection is to illustrate how the entropy production rate closure treats strong nonequilibrium away from the just discussed limit cases. For convenience, we introduce the dimensionless frequency $\xi = h\nu/k_B T$. First, we consider gray-matter (frequency independent $\kappa_\nu \equiv \kappa$) without scattering ($\sigma_\nu = 0$). In Fig. 1 a) the quantity $\xi^3 n$, being proportional to I_ν, is plotted as a function of ξ for $F = 0$ and three values of E, namely $E = E^{(eq)}$, $E = E^{(eq)}/2$, and $E = 2E^{(eq)}$. The first case corresponds the thermal equilibrium with $I_\nu = B_\nu$, while the others must have nonequilibrium populations of photon states. The results show that the energy unbalance is mainly due to under- and overpopulation, respectively, and only to a small extent due to a shift of the frequency maximum.

Now, consider a non-gray medium, still without scattering, but with a frequency dependent κ_ν as follows: $\kappa = 2\kappa_1$ for $\xi < 4$, with constant κ_1, and $\kappa = \kappa_1$ for $\xi > 4$. The important property is that κ_ν is larger at low frequencies and smaller at high frequencies. The resulting distribution function, in terms of $\xi^3 n$, is shown in Fig. 1 b). For $E = E^{(eq)}$, the resulting distribution is of course still the Planck equilibrium distribution. However, for larger (smaller) energy density the radiation density differs from the gray-matter case. In particular, the distribution is directly influenced by the κ_ν-spectrum. This behavior is not possible if one applies the maximum entropy closure in the same framework of a single-band moment approximation. A qualitative explanation of such behavior is as follows. Equilibration of the photon gas is only possible via the interaction with matter. In frequency bands where the interaction strength, κ_ν, is larger ($\xi < 4$), the nonequilibrium distribution is pulled closer to the equilibrium distribution than for frequencies with smaller κ_ν. This simple argument explains qualitatively the principal behavior associated with entropy production rate principles: the strength of the irreversible processes determines the distance from thermal equilibrium in the presence of a stationary constraint pushing a system out of equilibrium.

Results for the effective absorption coefficients $\kappa_E^{(\mathrm{eff})}$ and $\kappa_F^{(\mathrm{eff})}$ are shown in Fig. 2. In Fig. 2 a) it is shown that the effective absorption coefficient $\kappa_E^{(\mathrm{eff})}$ is equal to the Planck mean ($1.6\kappa_1$, dashed-double-dotted) in the emission limit $E/E^{(eq)} \to 0$, and equal to the Rosseland mean ($1.26\kappa_1$, dashed-dotted) near equilibrium $E = E^{(eq)}$, and eventually goes slowly to the high frequency value κ_1 for large E. The effective absorption coefficient obtained from the maximum entropy closure is also plotted (dotted curve), and although correct for $E/E^{(eq)} \to 0$,

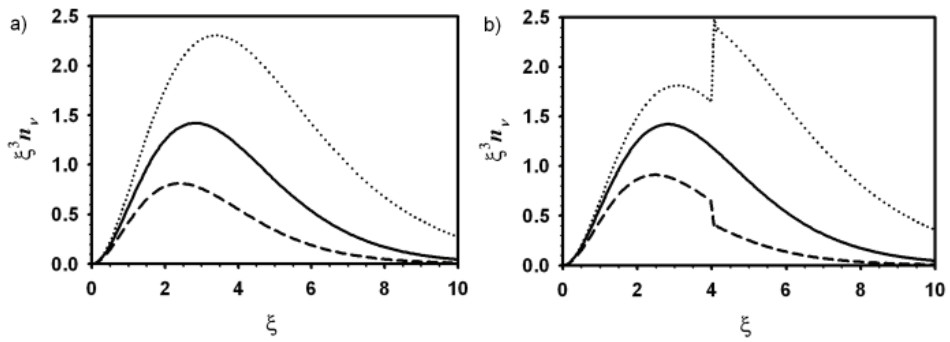

Fig. 1. Nonequilibrium distribution ($\xi^3 n_\nu \propto I_\nu$) as a function of $\xi = h\nu/k_B T$, without scattering, for $F = 0$ and $E = E^{(eq)}$ (solid), $E = E^{(eq)}/2$ (dashed), and $E = 2E^{(eq)}$ (dotted). a) gray matter; b) piecewise constant κ with $\kappa_{\xi<4} = 2\kappa_{\xi>4}$.

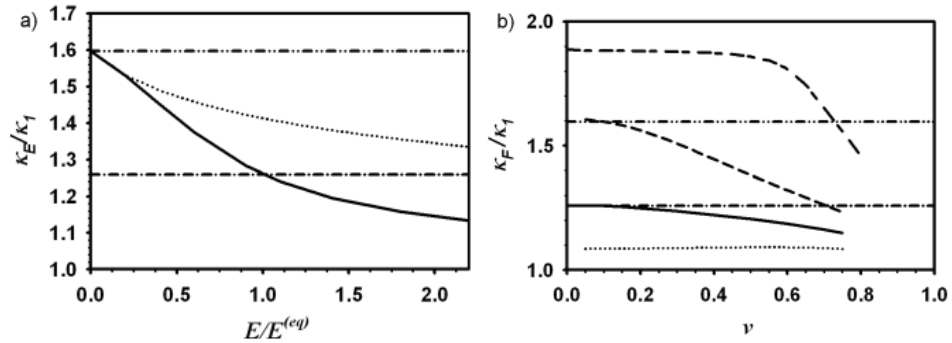

Fig. 2. a) Effective absorption coefficients for E as a function of E for $F = 0$, with the same spectrum as for Fig. 1 b). Dashed-dotted: Rosseland mean; dashed-double-dotted: Planck mean; solid: entropy production rate closure (correct at $E = E^{(eq)}$); dotted: entropy closure (wrong at $E = E^{(eq)}$). b) Effective absorption coefficients for **F** as a function of $v = F/E$ for different E-values (dotted: $E/E^{(eq)} = 2$; solid $E/E^{(eq)} = 1$; dashed: $E/E^{(eq)} = 0.5$; short-long dashed: $E/E^{(eq)} = 0.05$). Dashed-dotted and dashed-double dotted as in a).

it is wrong at equilibrium $E = E^{(eq)}$. For the present example the maximum entropy closure is strongly overestimating the values of $\kappa_E^{(\mathrm{eff})}$.

Figure 2 b) shows $\kappa_E^{(\mathrm{eff})}$ as a function v, for various values of E. As at constant E, increasing v corresponds to a shift of the distribution towards higher frequencies in direction of **F**, a decrease of $\kappa_E^{(\mathrm{eff})}$ must be expected, which is clearly observed in the figure.

In order to investigate the effect of scattering $\sigma_\nu \neq 0$, we consider the example of gray absorbing matter, i.e., constant $\kappa_\nu \equiv \kappa_1$, having a frequency dependent scattering rate $\sigma_{\xi<4} = 0$ and $\sigma_{\xi>4} = \kappa_1$. Scattering is only active for large frequencies. The distribution $\xi^3 n_\nu$ of radiation with $E = 2E^{(eq)}$, with finite flux $v = 0.25$ for different directions $\mu = \cos(\theta) = -1, -0.5, 0, 0.5, 1$ is plotted in Fig. 3 a). Since the total energy of the photon gas is twice the equilibrium energy, the curves are centered around about twice the equilibrium distribution. As one expects, the states in forward direction ($\mu = 1$) have the highest population, while the states propagating against the mean flux ($\mu = -1$) have lowest population. This behavior occurs, of course, also in the absence of scattering. One observes that scattering acts to decrease the anisotropy of the distribution, as for $\xi > 4$ the curves are pulled towards the state with $\mu \approx 0$. Hence, also the effect of elastic scattering to the distribution function can be understood in the framework of the entropy production, namely by the tendency to push the state towards equilibrium with a strength related to the interaction with the LTE matter.

The effective absorption coefficient $\kappa_F^{(\mathrm{eff})}$ is shown in Fig. 3 b) for two values of v; it is obvious that it must increase for increasing v and for increasing E. The Rosseland and Planck averages of $\kappa_\nu + \sigma_\nu$ are given by $1.42\kappa_1$ and $1.40\kappa_1$, while the emission limit for $\kappa_F^{(\mathrm{eff})}$ given in Eq. (47) is $1.20\kappa_1$.

The VEF will be discussed separately in the following subsection, because its behavior has not only quantitative physical, but also important qualitative mathematical consequences.

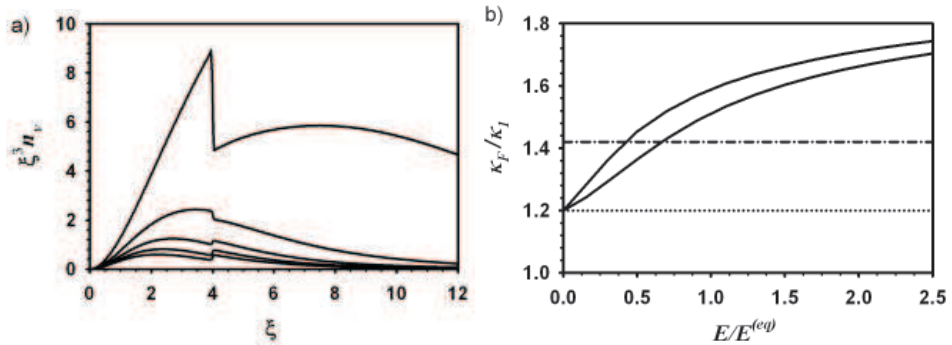

Fig. 3. a) Nonequilibrium distribution ($\xi^3 n_\nu \propto I_\nu$) as a function of $\xi = h\nu/k_B T$, for a medium with constant absorption $\kappa_\nu \equiv \kappa_1$ and piecewise constant scattering with $\sigma_{\xi<4} = 0$, and $\sigma_{\xi>4} = \kappa_1$. The different curves refer to different radiation directions of $\mu = -1, -0.5, 0, 0.5, 1$ (solid curves in ascending order) from photons counter-propagating to the mean drift **F** to photons in **F**-direction. b) Effective absorption coefficients $\kappa_F^{(\mathrm{eff})}$ as a function of $E/E^{(eq)}$ for $v = 0.25, 0.5$ (solid curves in ascending order); dashed-dotted: Rosseland mean, dashed: emission mean of $\kappa_F^{(\mathrm{eff})}$.

5.4 The variable Eddington factor and critical points

A detailed discussion of general mathematical properties and conventional closures is given by Levermore (1996). A necessary condition for a closure method is existence and uniqueness of the solution. It is well-known that convexity of a minimization problem is a crucial property in this context. One should note that convexity of the entropy production rate in nonequilibrium situations is often introduced as a presumption for further considerations rather than it is a proven property (cf. Martyushev (2006)). For the case without scattering, $\sigma_\nu \equiv 0$, Christen & Kassubek (2009) have shown that the entropy production rate (33) is strictly convex. A discussion of convexity for a finite scattering rate goes beyond the purpose of this chapter.

Besides uniqueness of the solution, the moment equations should be of hyperbolic type, in order to come up with a physically reasonable radiation model. It is an advantage of the entropy maximization closure that uniqueness and hyperbolicity are fulfilled and are related to the convexity properties of the entropy (cf. Levermore (1996)). In the following, we provide some basics needed for understanding the problem of hyperbolicity, its relation to the VEF and the occurrence of critical points. The latter is practically relevant because it affects the modelling of the boundary conditions, particularly in the context of numerical simulations. More details are provided by Körner & Janka (1992), Smit et al. (1997), and Pons et al. (2000).

A list of the properties that a reasonable VEF must have (cf. Pomraning (1982)) is: $\chi(v = 0) = 1/3$, $\chi(v = 1) = 1$, monotonously increasing $\chi(v)$, and the Schwarz inequality $v^2 \leq \chi(v)$. The latter follows from the fact that χ and v can be understood as averages of μ^2 and μ, respectively, with (positive) probability density $I_\nu(\mu)/E$. Hyperbolicity adds a further requirement to the list. Equations (13) and (14) form a set of quasilinear first order differential equations. For simplicity, we consider a one dimensional position space[5] with coordinate x with $0 \leq x \leq L$, and variables $E \geq 0$ and F. In this case we redefine F, such that it can have

[5]Momentum space remains three dimensional.

either sign, $-E \leq F \leq E$. We assume flux in positive direction, $F \geq 0$, and write the moment equations in the form

$$\frac{1}{c}\partial_t \begin{pmatrix} E \\ F \end{pmatrix} + \begin{pmatrix} 0 & 1 \\ \partial_E(\chi E) & E\partial_F \chi \end{pmatrix} \partial_x \begin{pmatrix} E \\ F \end{pmatrix} = \begin{pmatrix} P_E \\ P_F \end{pmatrix} . \tag{50}$$

For spatially constant E and F, small disturbances of δE and δF must propagate with well-defined speed, implying real characteristic velocities. Those are given by the eigenvalues of the matrix that appears in the second term on the left hand side of Eq. (50) and which we denote by $\mathbf{M}$:

$$w_\pm = \frac{\mathrm{Tr}\,\mathbf{M}}{2} \pm \sqrt{\frac{(\mathrm{Tr}\,\mathbf{M})^2}{4} - \det(\mathbf{M})} , \tag{51}$$

where "Tr" and "det" denote trace and determinant. Note that the $w_\pm$ are normalized to c, i.e. $-1 \leq w_- \leq w_+ \leq 1$ must hold. Hyperbolicity refers to real eigenvalues $w_\pm$ and to the existence of two independent eigenvectors. The condition for hyperbolicity reads $(\partial_F(\chi E))^2 + 4\partial_E(\chi E) > 0$.

Provided hyperbolicity is guaranteed, the sign of the velocities is an issue relevant for the boundary conditions. Indeed, the boundary condition, say at $x = L$, can only have an effect on the state in the domain if at least one of the characteristic velocities is negative. It is clear that a disturbance near equilibrium ($v = 0$) propagates in $\pm x$ direction since $w_+ = -w_-$ due to mirror symmetry. Hence $w_- < 0 < w_+$ for sufficiently small v. In this case boundary conditions to both boundaries $x = 0$ and $x = L$ have to be applied as in a usual boundary value problem. However, for finite v, reflection symmetry is broken and $w_+ \neq -w_-$. It turns out, that for sufficiently large v, either w_+ or w_- can change sign. For positive F, we denote the value of v where w_- becomes positive by v_c. This is called a *critical point* because $\det(\mathbf{M}) = w_+ w_-$ vanishes there. Beyond the critical point, all disturbances will propagate in positive direction, and a boundary condition at $x = L$ is not to be applied. This can introduce a problem in numerical simulations with fixed predefined boundary conditions. The rough physical meaning of the critical point is a cross-over from diffusion dominated to streaming dominated radiation. In the latter region it might be reasonable to improve the radiation model by involving higher order moments or partial moments, for example by decomposing the moments in backward and forward propagating components $E_\pm$ and $F_\pm$ (cf. sect. 3.1 in Frank (2007)).

In Fig. 4 a), different VEFs are shown. All of them exhibit the above mentioned properties, $\chi(v = 0) = 1/3$, monotonous increase, $\chi(v \to 1) = 1$, and the Schwarz inequality $v^2 \leq \chi$. In particular, the VEFs obtained from entropy production rate minimization is shown for $E = E^{(eq)}$ for gray matter with $\sigma_\nu \equiv 0$, as well as for the emission limit (cf. Eqs. (44) and (45)). Note that the latter $\chi(v)$ is a function of v only and is independent of the detailed properties of the absorption and scattering spectra. The similarity of the differently defined VEFs, combined with the error done anyhow by the two-moment approximation, makes it obvious that for practical purpose the simple Kershaw VEF ($j = 2$) may serve as a sufficient approximation. In Fig. 4 b) the characteristic velocities $w_\pm$ are plotted versus v for the various VEFs discussed above. It turns out that the VEF given by Eq. (25) has a critical point for $j > 3/2$ given by $v_c = 1/\sqrt[j]{2(j-1)}$, and that there is a minimum v_c value of 0.63 at $j = 3.16$. The VEF by Kershaw and maximum entropy have $v_c = 1/\sqrt{2}$ and $v_c = 2\sqrt{3}/5$, respectively. Also the VEF associated with the entropy production rate has generally a critical point, which depends on E. One has to expect a typical value of $v_c \approx 2/3$. For the VEF (25) with $j = 1$ a critical point does not

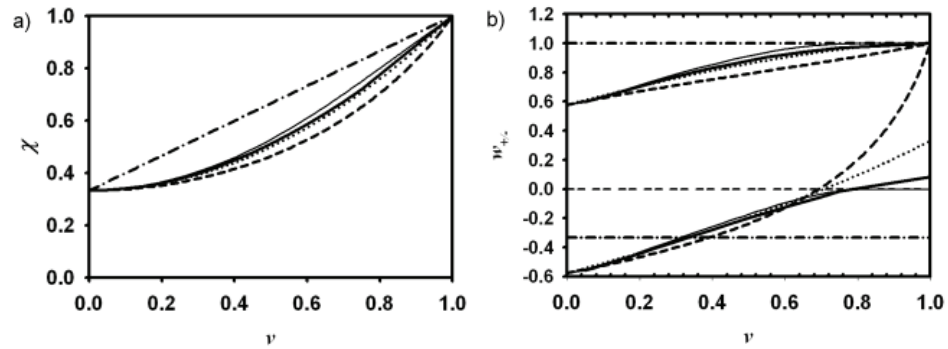

Fig. 4. a) Eddington Factors χ versus v and b) characteristic velocities $w_{\pm}$ for various cases. Minimum entropy production: $E = E^{(eq)}$ (thick solid curve) and emission limit $E \ll E^{(eq)}$ (thin solid curve); maximum entropy (dashed); Kershaw (dotted; $j = 2$ in Eq. (25)), and Auer (dashed-dotted; $j = 1$ in Eq. (25)).

appear. In the framework of numerical simulations, this advantage can outweigh in certain situations the disadvantage of the erroneous anisotropy in the $v \to 0$ limit.

6. Boundary conditions

In order to solve the moment equations, initial and boundary conditions are required. While the definition of initial conditions are usually unproblematic, the definition of boundary conditions is not straight-forward and deserves some remarks. In the sequel we will consider boundaries where the characteristic velocities are such that boundary conditions are needed. But note that the other case where boundary conditions are obsolete can also be important, for example in stellar physics where, beyond a certain distance from a star, freely streaming radiation completely escapes into the vacuum.
The mathematically general boundary condition for the two-moment model is of the form

$$aE + b\hat{\mathbf{n}} \cdot \mathbf{F} = \Gamma \ , \tag{52}$$

with the surface normal $\hat{\mathbf{n}}$, and where the coefficients a, b, and the inhomogeneity Γ must be determined from Eq. (5). There is a certain ambiguity to do this (cf. Duderstadt & Martin (1979)) and thus a number of different boundary conditions exist in the literature (cf. Su (2000)).
There may be simple cases where one can either apply Dirichlet boundary conditions $E(\mathbf{x}_{\mathrm{w}}) = E_{\mathrm{w}}$ to E, where E_{w} is the equilibrium value associated with the (local) wall temperature, and/or homogeneous Neumann boundary conditions to $\mathbf{F}$, $(\hat{\mathbf{n}} \cdot \nabla)\mathbf{F} = 0$, at $\mathbf{x}_{\mathrm{w}}$. This approach may be appropriate, if the boundaries do not significantly influence the physics in the region of interest, e.g., in the case where cold absorbing boundaries are far from a hot radiating object under investigation. It can also be convenient to include in the simulation, instead of using boundary conditions, the solid bulk material that forms the surface, and to describe it by its κ_ν and σ_ν. In the next section an example of this kind will be discussed. If necessary, thermal equilibrium boundary conditions deep inside the solid may be assumed. In this way, it is also possible to analytically calculate the Stefan-Boltzmann radiation law for a plane sandwich structure (hot solid body)-(vacuum gap)-(cold solid body), if an Eddington factor (25) with $j = 1$ is used and the solids are thick opaque gray bodies.

In general, however, one would like to have physically reasonable boundary conditions at a surface characterized by Eq. (5). For engineering applications, often boundary conditions by Marshak (1947) are used. In the following, we sketch the principle how these boundary conditions can be derived for a simple example (cf. Bayazitoglu & Higenyi (1979)). For other types, like Mark or modified Milne boundary conditions see, e.g. Su (2000). Let the coordinate $x \geq 0$ be normal to the surface at $x = 0$, and ask for the relation between the normal flux F, E, and $E_{\mathrm{w}}^{(eq)}$ at $x = 0$. The $\mathbf{F}$-components tangential to the boundary are assumed to vanish, and diffusive reflection with $r(\mathbf{x_w}, \mathbf{\Omega}, \tilde{\mathbf{\Omega}}) = r/\pi$ with $r = 1 - \epsilon$ is considered. In terms of moments, the radiation field is given by

$$I_\nu = \frac{c}{4\pi}\left(E_\nu P_0(\mu) + 3F_\nu P_1(\mu) + \frac{5}{2}(3\Pi_{\nu,11} - E_\nu)P_2(\mu) + ...\right) \ , \tag{53}$$

with Legendre polynomials $P_0 = 1$, $P_1 = \mu$, $P_2 = (3\mu^2 - 1)/2$. The exact solution contains also higher order Legendre polynomials, as indicated by the dots. The boundary condition (5) can be written as

$$I_\nu(\mu \geq 0) = \epsilon B_\nu + 2r \int_{-1}^{0} d\tilde{\mu} \mid \tilde{\mu} \mid I_\nu(\tilde{\mu}) \ . \tag{54}$$

By using Eq. (53), the integral can be calculated, such that the right hand side of Eq. (54) becomes a constant with respect to μ, while the left hand side is, according to Eq. (53), a function of μ defined for $0 \leq \mu \leq 1$. In order to obtain the required relation between F and E, one has to multiply Eq. (54) with a weight function $h(\mu)$ and integrate over μ from 0 to 1. The above mentioned ambiguity lies in the freedom of choice of $h(\mu)$. Marshak (1947) selected $h = P_1$. Provided P_n for $n > 3$ are neglected in Eq. (53), integration leads to an inward flux

$$F = \frac{\epsilon}{2(2-\epsilon)}\left(E_{\mathrm{w}} - \frac{(3E + 15\Pi_{11})}{8}\right) \ , \tag{55}$$

where $\Pi_{11} = \chi E$. If higher order moments are to be considered, additional projections have to be performed, in analogy to the procedure reported by Bayazitoglu & Higenyi (1979) for the P-3 approximation.[6] For isotropic radiation with $\chi = 1/3$, or $\Pi_{11} = E/3$, the prefactor of E becomes unity and Eq. (55) reduces to the well-known P-1-Marshak boundary condition. In the transparent limit with $\chi = 1$, the prefactor becomes $9/4$.

For the simple case of two parallel plane plates ($\epsilon = 1$) with temperatures associated with $E_{\mathrm{w},1}$ and $E_{\mathrm{w},2} < E_{\mathrm{w},1}$, and separated by a vacuum gap, both moments E and F are spatially constant and the Stefan-Boltzmann law $F = (E_1^{(eq)} - E_2^{(eq)})/4$ is recovered. But note that the energy density E between the plates is not equal to the expected average of $E_1^{(eq)}$ and $E_2^{(eq)}$, which is an artifact of the two-moment approximation with VEF.

7. A simulation example: electric arc radiation

The two-moment approximation will now be illustrated for the example of an electric arc. The extreme complexity of the full radiation hydrodynamics is obvious. Besides transonic and turbulent gas dynamics, which is likely supplemented with side effects like mass ablation and electrode erosion, a temperature range between room temperature and up to 30′000K

[6] Note that neither the series (53) stops after the N'th moment (even not for the P-N approximation, cf. Cullen (2001)), nor all higher order coefficients drop out after projection of Eq. (54) on P_n. A general discussion, however, goes beyond this chapter and will be published elsewhere.

is covered. In this range extremely complicated absorption spectra including all kinds of transitions occur, and the radiation is far from equilibrium although the plasma can often be considered at LTE. Last but not least, the geometries are usually of complicated three-dimensional nature without much symmetry, as for instance in a electric circuit breaker. More details are given by Jones & Fang (1980), Aubrecht & Lowke (1994), Eby et al. (1998), Godin et al. (2000), Dixon et al. (2004), and Nordborg & Iordanidis (2008).

It is sufficient for our purpose to restrict the considerations to the radiation part for a given temperature profile, for instance of a cylindrical electric arc in a gas in front of a plate with a slit (see Fig. 5). We may neglect scattering in the gas ($\sigma_\nu \equiv 0$) and mention that an electric arc consists of a very hot, emitting but transparent core surrounded by a cold gas, which is opaque for some frequencies and transparent for others. First, one has to determine the effective transport coefficients $\kappa_E^{(\mathrm{eff})}$, $\kappa_F^{(\mathrm{eff})}$, and $\chi(v)$, with the above introduced entropy production minimization method. For simplicity, we assume now that this is done and these functions are given simply by constant values listed in the caption of Fig. 5, and that $\chi(v)$ is well-approximated by Kershaw's VEF. Note that due to the low density in the hot arc core, the effective absorption coefficient there is smaller than in the surrounding cold gas. Therefore, one expects that the radiation in the arc center will exhibit stronger nonequilibrium than in the surrounding colder gas.

The energy density E and the velocity vectors $\mathbf{v} = \mathbf{F}/E$ obtained by a simulation with the commercial software ANSYS® FLUENT® are shown in Fig. 5. At the outer boundaries, homogeneous Neumann boundary conditions are used for all quantities. The wall defining the slit is modelled as a material with either a) high absorption coefficient or b) high scattering coefficient. The behavior of the velocity vector field clearly reflects these different boundary properties. The E-surface plot shows the shadowing effect of the wall when the arc radiation is focused through the slit. The energy densities E along the x-axis are shown in Fig. 6 a) for the two cases. One observes the enhanced E in the region of the slit for the scattering wall. The energy flux in physical units, i.e., cF, on the screen in front of the slit is shown in Fig. 6 b). The effect here is again what one expects: an enhanced and less focused power flux due to the absence of absorption in the constricting wall.

8. Summary and conclusion

After a short general overview on radiative heat transfer, this chapter has focused on truncated moment expansions of the RTE for radiation modelling. One reason for a preference of a moment based description is the occurrence of the moments directly in the hydrodynamic equations for the matter, and the equivalence of the type of hyperbolic partial differential equations for radiation and matter, which allows to set complete numerical simulations on an equal footing.

The truncation of the moment expansion requires a closure prescription, which determines the unknown transport coefficients and provides the nonequilibrium distribution as a function of the moments. It was the main goal of this chapter to introduce the minimum entropy production rate closure, and to illustrate with the help of the two-moment approximation that this closure is the one to be favored due to the following properties of the result:

– It is exact near thermodynamic equilibrium, and particularly leads to the Rosseland mean absorption coefficients.
– It exhibits the required flux limiting behavior by yielding reasonable variable Eddington factors.

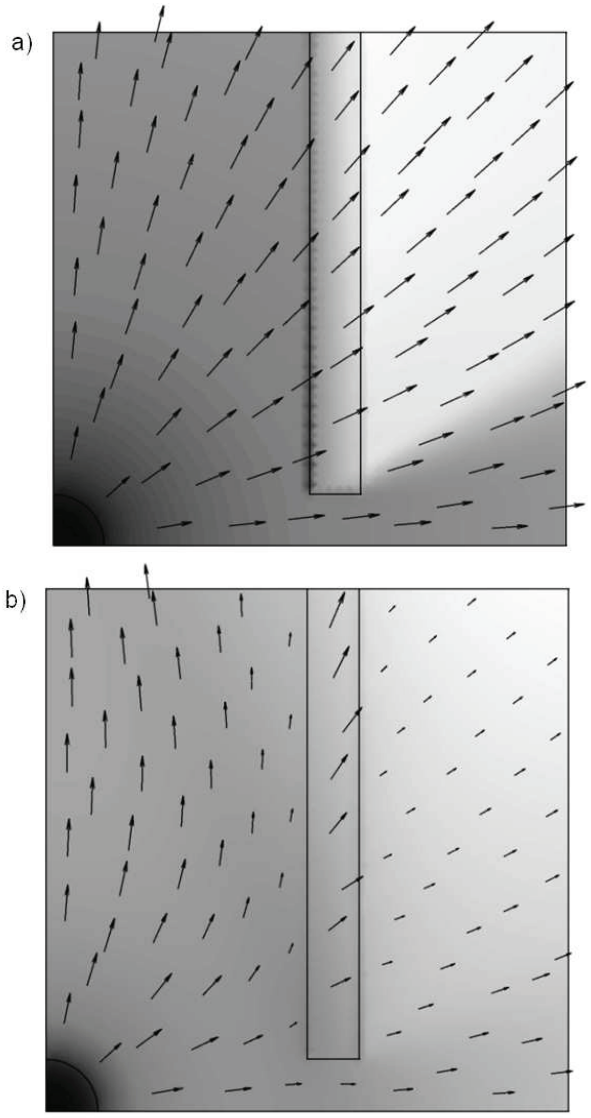

Fig. 5. Illustrative simulations of the moment equations with FLUENT® for a cylindrical electrical arc (radius 1 cm, temperature 10′000 K, $\kappa_E^{(\mathrm{eff})} = \kappa_F^{(\mathrm{eff})} = 1/\mathrm{m}$) in a gas (ambient temperature 300 K, $\kappa_E^{(\mathrm{eff})} = \kappa_F^{(\mathrm{eff})} = 5/\mathrm{m}$). A solid wall (a): only absorbing with $\kappa_E^{(\mathrm{eff})} = \kappa_F^{(\mathrm{eff})} \equiv 500/\mathrm{m}$; (b): wall with scattering coefficient, and $\kappa_E^{(\mathrm{eff})} = 5/\mathrm{m}$, $\kappa_F^{(\mathrm{eff})} \equiv 500/\mathrm{m}$ with a slit in front of the arc focusing the radiation towards a wall. Surface plot for E (dark: large, bright: small, logarithmic scale); arrows for $\mathbf{v}$ (not $\mathbf{F}$!). Only one quadrant of the symmetric arrangement is show.

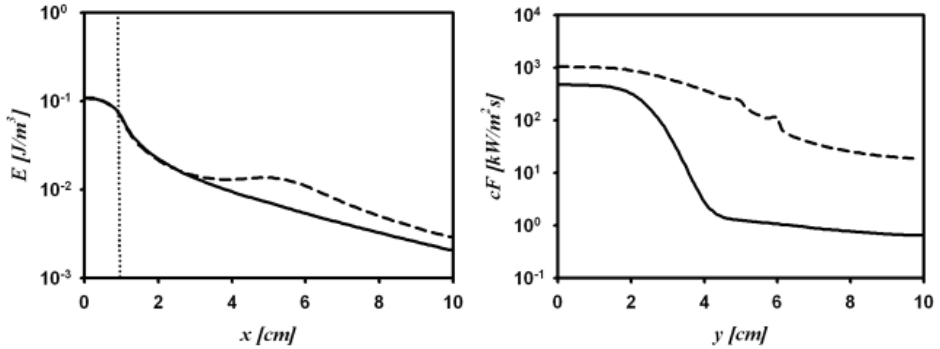

Fig. 6. a) Energy density along the x-axis (arc center at $x = 0$) and b) power flux along the screen ($x = 10$cm) for the two cases Fig. 5 a) (solid) and Fig. 5 b) (dashed).

- It gives the expected results in the emission limit, and particularly leads to the Planck mean absorption coefficient.
- It can be generalized to an arbitrary number and type of moments.
- It can be generalized to particles with arbitrary type of energy-momentum dispersion (e.g. massive particles) and statistics (Bosons and Fermions), as long as they are described by a linear BTE. In stellar physics, for instance, neutrons or even neutrinos can be included in the analogous way.

The main requirement of general applicability is that the particles be independent, i.e., they interact on the microscopic scale only with a heat bath but not among each other. On a macroscopic scale, long-range interaction (e.g., Coulomb interaction) via a mean field may be included for charged particles on the hydrodynamic level of the moment equations. Independency, i.e. linearity of the underlying Boltzmann equation, has the effect that on the level of the BTE (or RTE) nonequilibrium is always in the linear response regime. In this sense, all transport steady-states are near equilibrium even if f_ν strongly deviates from $f_\nu^{(eq)}$, and the entropy production rate optimization according to Kohler (1948) can be applied.

9. References

Abu-Romia M M and Tien C L, *J. Heat Transfer* 89, 321 (1967).
Anile A M, Pennisi S, and Sammartino M, *J. Math. Phys.* 32, 544 (1991).
Anile A, Romano V, and Russo G, *SIAM J. Appl. Math.* 61, 74 (2000).
Arridge S. R. et al., *Med. Phys.* 27, 252 (2000).
Aubrecht V, Lowke J J, *J. Phys. D: Appl. Phys.* 27, 2066 (1994).
Auer L H, in *Methods in radiative transfer*, ed. Kalkofen W, Cambridge University Press (1984).
Barichello L B and Siewert C E, *Nuclear Sci. and Eng.* 130,79 (1998).
Bayazitoglu Y and Higenyi J, *AIAA Journal* 17, 424 (1979).
Brooks E D and Fleck A, *J. Comp. Phys.* 67, 59 (1986).
Brooks E D et al. *J. Comp. Phys.* 205, 737 (2005).
Cernohorsky J and Bludman S A, *The Astrophys. Jour.* 443, 250 (1994).
Chandrasekhar S, *Radiative Transfer*, Dover Publ. Inc., N. Y. (1960).
Christen T, *J. Phys. D: Appl. Phys.* 40, 5719 (2007).
Christen T and Kassubek F, *J. Quant. Spectrosc. Radiat. Transfer.*110, 452 (2009).

Christen T *Entropy* 11, 1042 (2009).
Christen T, *Europhys. Lett.* 89, 57007 (2010).
Cullen D E and Pomraning G C, *J. Quant. Spectrosc. Radiat. Transfer.* 24, 97 (1980).
Cullen D E, *Why are the P-N and the S-N methods equivalent?*, UCRL-ID-145518 (2001).
Dixon C M, Yan J D, and Fang M T C, *J. Phys. D: Appl. Phys* 37, 3309 (2004).
Duderstadt J J and Martin W R, *Transport Theory*, Wiley Interscience, New York (1979).
Eby S D, Trepanier J Y, and Zhang X D, *J. Phys. D: Appl. Phys.* 31, 1578 (1998).
Essex C, *The Astrophys. Jeut.* 285, 279 (1984).
Essex C, *Minimum entropy production of neutrino radiation in the steady state*, Institute for fundamental theory, UFIFT HEP-97-7 (1997).
Fort J, *Physica A* 243, 275 (1997).
Frank M, Dubroca B, and Klar A, *J. Comput. Physics* 218, 1 (2006).
Frank M, *Bull. Inst. Math. Acad. Sinica* 2, 409 (2007).
Fuss S P and Hamins A, *J. Heat Transfer ASME* 124, 26 (2002).
Godin D et al., *J. Phys. D: Appl. Phys* 33, 2583 (2000).
Jones G R and Fang M T C, *Rep. Prog. Phys.* 43, 1415 (1980).
Kabelac S, *Thermodynamik der Strahlung* Vieweg, Braunschweig (1994).
Kershaw D, *Flux limiting nature's own way*, Lawrence Livermore Laboratory, UCRL-78378 (1976).
Kohler M, *Z. Physik* 124, 772 (1948).
Körner A and Janka H-T, *Astron. Astrophys.* 266, 613 (1992).
Kröll W, *J. Quant. Spectrosc. Radiat. Transfer.* 7, 715 (1967).
Landau L D and Lifshitz E M, *Statistical Physics*, Elsevier, Amsterdam (2005).
Levermore C D, *J. Quant. Spectrosc. Radiat. Transfer.* 31, 149 (1984).
Levermore C D, *J. Stat. Phys.* 83, 1021 (1996).
Levermore C D and Pomraning G C, *The Astrophys. Jou. Y* 248, 321 (1981).
Lowke J J, *J. Appl. Phys.* 41, 2588 (1970).
Marshak R E, *Phys. Rev.* 71, 443 (1947).
Martyushev L M and Seleznev V D, *Phys. Rep.* 426, 1 (2006).
Minerbo G N, *J. Quant. Spectrosc. Radiat. Transfer.* 20, 541 (1978).
Mihalas D and Mihalas B W, *Foundations of Radiation Hydrodynamics*, Oxford University Press, New York (1984).
Modest M, *Radiative Heat Transfer*, Elsevier Science, (San Diego, USA, 2003).
Nordborg H and Iordanidis A A, *J. Phys. D: Appl. Phys.* 41, 135205 (2008).
Olson G L, Auer L H, and Hall M L, *J. Quant. Spectrosc. Radiat. Transfer.* 64, 619 (2000).
Oxenius J, *J. Quant. Spectrosc. Radiat. Transfer.* 6, 65 (1966).
Patch R W, *J. Quant. Spectrosc. Radiat. Transfer.* 7, 611 (1967).
Planck M, *Vorlesungen über die Theorie der Wärmestrahlung*, Verlag J. A. Barth, Leipzig (1906).
Pons J A, Ibanez J M, and Miralles J A, *Mon. Not. Astron. Soc.* 317, 550 (2000).
Pomraning G C, *J. Quant. Spectrosc. Radiat. Transfer.* 26, 385 (1981).
Pomraning G C, *Radiation Hydrodynamics* Los Alamos National Laboratory, LA-UR-82-2625 (1982).
Rey C C, *Numerical Methods for radiative transfer*, PhD Thesis, Universitat Politecnica de Catalunya (2006).
Ripoll J-F, Dubroca B, and Duffa G, *Combustion Theory and Modelling* 5, 261 (2001).
Ripoll J-F , *J. Quant. Spectrosc. Radiat. Transfer.* 83, 493 (2004).
Ripoll J-F and Wray A A, *J. Comp. Phys.* 227, 2212 (2008).

Sampson D H, *J. Quant. Spectrosc. Radiat. Transfer.* 5, 211 (1965).
Santillan M, Ares de Parga G, and Angulo-Brown F, *Eur. J. Phys.* 19, 361 (1998).
Seeger M, et al. *J. Phys. D: Appl. Phys* 39, 2180 (2006).
Siegel R and Howell J R, *Thermal radiation heat transfer*, Washington, Philadelphia, London; Hemisphere Publ. Corp. (1992).
Simmons K H and Mihalas D, *J. Quant. Spectrosc. Radiat. Transfer.* 66, 263 (2000).
Smit J M, Cernohorsky J, and Dullemond C P *Astron. Astrophys.* 325, 203 (1997).
Struchtrup H, *Ph. D. Thesis* TU Berlin (1996).
Struchtrup H, in *Rational extended thermodynamics* ed. Müller I. and Ruggeri T., Springer, New. York, Second Edition, p. 308 (1998).
Su B, *J. Quant. Spectrosc. Radiat. Transfer.* 64, 409 (2000).
Tien C L, *Radiation properties of gases*, in *Advances in heat transfer*, Vol.5, Academic Press, New York (1968).
Turpault R, *J. Quant. Spectrosc. Radiat. Transfer.* 94, 357 (2005).
Würfel P and Ruppel W, *J. Phys. C: Solid State Phys.* 18, 2987 (1985).
Yang W-J, Taniguchi H, and Kudo K, *Radiative Heat Transfer by the Monte Carlo Method*, Academic Press, San Diego (1995).
Ziman J M, *Can. J. Phys.* 34, 1256 (1956).
Zhang J F, Fang M T C, and Newland D B, *J. Phys. D: Appl. Phys* 20, 368 (1987).

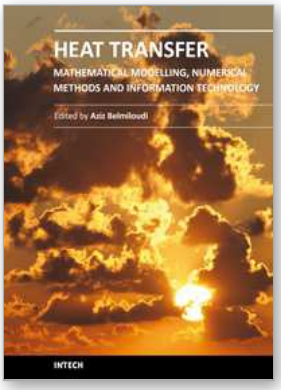

Heat Transfer - Mathematical Modelling, Numerical Methods and Information Technology

Edited by Prof. Aziz Belmiloudi

ISBN 978-953-307-550-1
Hard cover, 642 pages
Publisher InTech
Published online 14, February, 2011
Published in print edition February, 2011

Over the past few decades there has been a prolific increase in research and development in area of heat transfer, heat exchangers and their associated technologies. This book is a collection of current research in the above mentioned areas and describes modelling, numerical methods, simulation and information technology with modern ideas and methods to analyse and enhance heat transfer for single and multiphase systems. The topics considered include various basic concepts of heat transfer, the fundamental modes of heat transfer (namely conduction, convection and radiation), thermophysical properties, computational methodologies, control, stabilization and optimization problems, condensation, boiling and freezing, with many real-world problems and important modern applications. The book is divided in four sections : "Inverse, Stabilization and Optimization Problems", "Numerical Methods and Calculations", "Heat Transfer in Mini/Micro Systems", "Energy Transfer and Solid Materials", and each section discusses various issues, methods and applications in accordance with the subjects. The combination of fundamental approach with many important practical applications of current interest will make this book of interest to researchers, scientists, engineers and graduate students in many disciplines, who make use of mathematical modelling, inverse problems, implementation of recently developed numerical methods in this multidisciplinary field as well as to experimental and theoretical researchers in the field of heat and mass transfer.

How to reference

In order to correctly reference this scholarly work, feel free to copy and paste the following:

Thomas Christen, Frank Kassubek and Rudolf Gati (2011). Radiative Heat Transfer and Effective Transport Coefficients, Heat Transfer - Mathematical Modelling, Numerical Methods and Information Technology, Prof. Aziz Belmiloudi (Ed.), ISBN: 978-953-307-550-1, InTech, Available from: http://www.intechopen.com/books/heat-transfer-mathematical-modelling-numerical-methods-and-information-technology/radiative-heat-transfer-and-effective-transport-coefficients

INTECH
open science | open minds

InTech Europe
University Campus STeP Ri
Slavka Krautzeka 83/A
51000 Rijeka, Croatia
Phone: +385 (51) 770 447

InTech China
Unit 405, Office Block, Hotel Equatorial Shanghai
No.65, Yan An Road (West), Shanghai, 200040, China
中国上海市延安西路65号上海国际贵都大饭店办公楼405单元
Phone: +86-21-62489820

Fax: +385 (51) 686 166
www.intechopen.com

Fax: +86-21-62489821